World Conference on Timber Engineering Oslo 2023

QUASI-STATIC CYCLIC TESTS OF NOVEL HIGH-PERFORMANCE SHEAR-CONNECTORS FOR MASS-TIMBER PANELS

Blériot V. Feujofack K.[1], Cristiano Loss[2]

ABSTRACT: In this work, the results from quasi-static cyclic tests on a novel hybrid steel-grout shear connector for cross-laminated timber (CLT) panels is presented. These tests are part of a set of experimental, analytical, and numerical studies aiming at developing a reliable and resilient hold-down connection for CLT panels in mass-timber construction. The cyclic tests have been done based on monotonic-test results, and all cyclic loading was done below the yield point of each connector. From cyclic-test results, mechanical characteristics, namely, the secant loading stiffness and the residual slip were evaluated and are discussed in this paper. Furthermore, analyses using a Gaussian process regression machine learning algorithm were conducted in order to predict the mechanical characteristics of connectors in function of a vast number of inputs, including geometrical properties of connectors, mechanical properties of each material used, and physical parameters such as the position of lumber laminates in the CLT. It was shown that the steel rod diameter, the grout diameter, and the curing time of the grout are the most influencing parameters regarding the secant loading stiffness of connectors. As for the residual slip, it was found that the grout diameter, the steel rod grade, and the position of face-laminate joints in the CLT are the most influencing parameters. In overall, the results of this work contribute to an improved understanding of the connection under development and confirms the resilience of individual connectors under cyclic loads.

KEYWORDS: CLT, Hybrid steel-grout connector, Quasi-static cyclic, Hysteresis, Secant loading stiffness, Residual slip, Gaussian process regression algorithm, machine learning

1 INTRODUCTION

Mass timber construction is increasingly growing attention among architects, engineers, and other practitioners. Factors such as ease of hybridization, high sustainability potential, along with the better performance of mass timber products under fire motivate building regulators to relax timber buildings' height limitations around the world. For instance, timber buildings can now reach up to 25 m in Australia; 12 stories in Canada; and 18 stories in the USA [1]. Although the development of novel mass-timber products and hybrid timber-based systems can result in high-performance solutions for tall buildings, the structural efficiency of those buildings heavily depends on the connection technologies employed. Various connection technologies have to be reinvented in order to suit the needs of mass-timber construction, among which dowelled hold-downs connections. Research has already been initiated for such connection technologies [2]. The few solutions proposed remain very embryonic, and the observed performance are not always satisfactory, as brittle failure in wood is engaged before developing yielding in the connectors. Therefore, the need for reliable, resilient, and high-performance dowel-type connection technologies for mass timber components is becoming increasingly critical. In this work, the results of quasi-static cyclic tests on a novel hybrid steel-grout shear connector for cross-laminated timber (CLT) panels are presented. Precisely, this work is part of a research program aiming at developing a reliable and resilient hold-down connection for CLT panels in mass timber construction.

2 METHODS

2.1 Description of the hybrid connector

The hybrid shear connector developed and tested in this work consists of a threaded steel rod embedded into cross-laminated timber (CLT) through a thick layer of epoxy-based grout mixture. With specific reference to Figure 1, each connector unit includes:

- A steel threaded rod, which ensures the transfer of shear forces from side members to the connector and conversely. In this study, three steel rod diameters were used and tested, namely 20 mm, 24 mm, and 30 mm. Additionally, two steel rod grades were accounted for, namely 4.8 strength class and 8.8 strength class.

[1] Blériot V. Feujofack K., Ph.D. Candidate, Sustainable Engineered Structural Solutions Laboratory, Department of Wood Science, The University of British Columbia, Canada; bleriotvincent.feujofackkemda@ubc.ca

[2] Cristiano Loss, Assistant Professor, Sustainable Engineered Structural Solutions Laboratory, Department of Wood Science, The University of British Columbia, Canada; cristiano.loss@ubc.ca

https://doi.org/10.52202/069179-0174

• An intermediary thick layer of epoxy-based grout, which enables to embed the threaded rod into the CLT panel (wood). More importantly, this intermediary layer of epoxy-based grout enables to reduce stress and strain on wood, delaying crushing and failure in wood to a great extent. In the current study, the diameter of the grout was varied in function of the diameter of steel threaded rods. The grout-to-rod diameter ratio was set to 2, 3, and 4.

• A CLT block, into which the steel rod and the grout layer are embedded. A 3-ply CLT with fixed thickness of 105 mm was studied. Two CLT grades were used, namely machine graded CLT (E), and visually graded CLT (V). In addition, the CLT block size was varied from 280 mm to 340 mm, to 420 mm, in function of the diameter of steel threaded rods used.

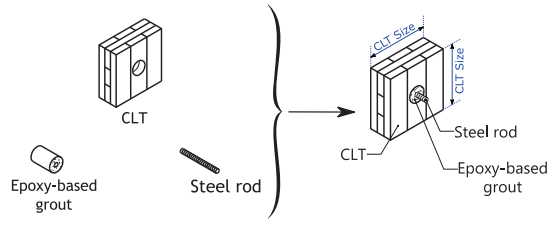

Figure 1: *Individual components (left); the hybrid steel-grout connector (right) for CLT panels*

Shulman and Loss [3], [4] conducted an extensive experimental campaign on this connector and provided insights on the actual structural performance of such connectors under monotonic loading.

2.2 Rationale for conduction of cyclic testing

The shear connector presented in this work is expected to be wood-damage-free and de-constructable. For such goals to be attained, it is important for the connector to remain elastic throughout the building lifespan. For static loading, the connector has been proven to display a high slip modulus and a clearly identifiable yield point [5]. However, repeated cyclic loads can lead to permanent deformation into the connector, even for small load amplitudes. Given that buildings are often subjected to recurrent cyclic loading such as regular winds or gusts, and sometimes earthquakes, it is important to determine the behaviour of the connector under repeated cyclic loading.

In the aim of determining the mechanical properties of the connector when subjected to cyclic loads, load-controlled quasi-static cyclic non-reversed tests were conducted on connectors. The tests were non-reversed, because in the scenario where connectors are used in hold-down connections, each connector is loaded in one direction only: the full reverse of loads does not occur for individual connectors. Three replicates of all the variants tested by Shulman and Loss [3], [4] were fabricated under the same condition and stored for at least seven days, before proceeding to testing. The testing campaign was set to evaluate to what extent cyclic loading, below the connector's yield strength, negatively impacts the connector strength, stiffness, and overall integrity.

2.3 Testing program

2.3.1 Design of experiments

The size of specimens and testing method were set based on monotonic-test results conducted in early 2021 by Shulman and Loss [3], [4]. Cyclic tests were load-controlled, and the amplitude of cycling was kept below the yield point for each connector. As shown in Figure 2, experimental variables include the grade of the CLT panel, the diameter of the steel threaded rod, the strength class of the steel threaded rod, and the ratio between the grout diameter and the steel rod diameter. The combination of all experimental variables yielded a total of 30 connector variants. Each test was replicated thrice, leading to a total of 90 tests for this study.

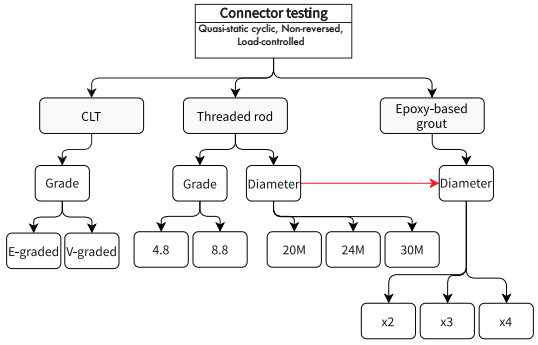

Figure 2: *Experimental variables and their associated levels*

2.3.2 Loading protocol for cyclic testing

The loading protocol was crafted from European [6] and American [7] standards. For each connector variant, the reference maximum load ($\boldsymbol{F_{max-cyclic}}$) was set as the average yield load ($F_{y,mean}$) obtained from monotonic tests by S. Shulman and C. Loss [3], [4]. Then, cyclic loads were applied on connectors by steps, at 5%, 20%, 40%, 60%, 80%, 90%, and 100% of $F_{y,mean}$. Figure 3 shows a graphic of that loading protocol. Specifically, only one cycle was applied at the first load step. For each subsequent load step, five non-reversed loading cycles were applied. The loading speed was set at one cycle per two minutes, for a total of 62 minutes per test. Figure 3 presents the loading protocol of the connector variant 280–E–20M–4.8–2d. Table 1 shows the characteristics of this connector variant such as the CLT block size and grade, the steel rod diameter and grade and the grout diameter; each load step, as well as number of cycles per steps are also provided.

https://doi.org/10.52202/069179-0174

***Table 1**: Loading protocol sample*

Specimen: 280 – E – 20M – 4.8 – 2d				
CLT size	CLT grade	Rod diameter (d)	Steel class (rod)	Grout diameter
280 mm	E	20M	4.8	2d

$$F_{max-cyclic} = F_y = 74.58\ kN$$

Loading schedule

Steps	Number of cycles	Load percentage (%)	Actual load (kN)	Loading speed (kN/min)	Total time (min)
1	1	5	3.73	3.73	2
2	5	20	14.92	14.92	10
3	5	40	29.83	29.83	10
4	5	60	44.71	44.71	10
5	5	80	59.67	59.67	10
6	5	90	67.13	67.13	10
7	5	100	74.58	74.58	10
Total					62

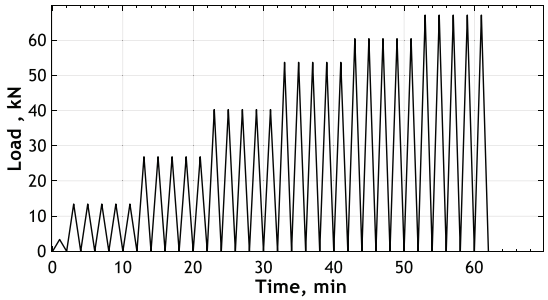

***Figure 3:** Graphic representation of the loading protocol*

All tests were conducted in the Timber Structural and Mechanical Lab at the University of British Columbia, using a custom-made test apparatus, as shown in Figure 4. Throughout the tests, the load was measured and recorded using the built-in load cell of the MTS machine. The slip of the connector was measured with two linear voltage displacement transducers and recorded using a standard data acquisition system. The load and slip data were acquired with a frequency of 4 Hz. Furthermore, physical and environmental variables such as moisture content of the CLT were duly recorded during the tests. In addition to the geometry and mechanical properties of the steel threaded rod, the layer of epoxy-based grout, and the CLT block, parameters such as the number of knots in the loaded end of the CLT and the position of the connector with respect to edge joints in the CLT face lamellae (Figure 5) were recorded as covariate for the predictive models to be developed. The parameter d_1 represents the horizontal eccentricity: it was measured as the perpendicular distance between the vertical axis of the steel threaded rod and the closest face lamination (major) joint of the CLT block. As for d_2, it represents the vertical eccentricity: it is the perpendicular distance between the horizontal axis of the steel threaded rod and the closest lower internal-laminate (minor) joint.

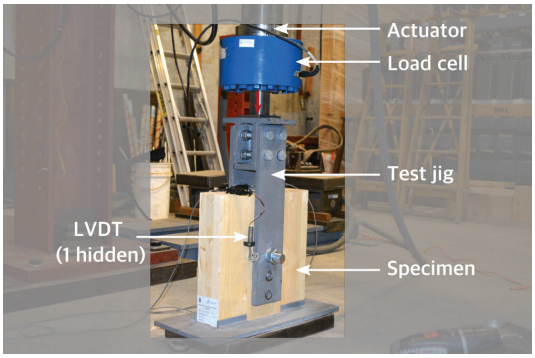

***Figure 4:** Experimental test apparatus*

***Figure 5:** Characterization of the location of the connector in the CLT panel, and defects in the panel*

2.4 Evaluation of structural performance parameters

Based on the experimental tests conducted, a set of parameters have been selected to characterize the structural performance of connectors, namely, the secant loading stiffness (k_{sl}), and the residual slip of the connector and the end of the cycling process ($\delta_{res-slip}$). These structural performance parameters are represented in an idealized hysteresis plot in Figure 6.

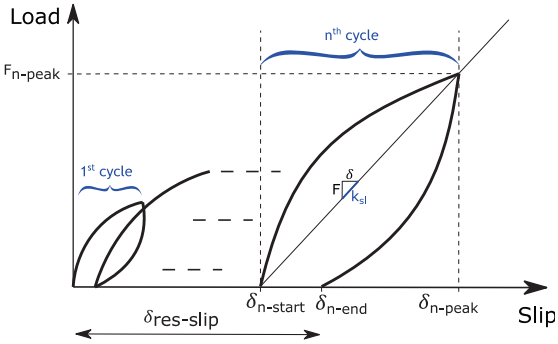

***Figure 6:** Idealised hysteresis curves of the connector and identification of performance parameters.*

https://doi.org/10.52202/069179-0174

With specific reference to Figure 6, the secant loading stiffness for a given cycle n was determined using equation 1 [8], [9].

$$k_{sl} = \frac{F_{n-peak} - F_{n-start}}{\delta_{n-peak} - \delta_{n-start}} \quad (1)$$

Where $\delta_{n-start}$ and δ_{n-peak} correspond to the recorded connector slip at the starting and ending of the load cycle n, respectively. $F_{n-start}$ and F_{n-peak} correspond to the recorded load at the starting and ending of the load cycle n, respectively. In this study, the final value of k_{sl} considered was obtained by averaging the secant loading stiffness of the last five cycles of each test-run. For what ensues, k_{sl} will be referred to as loading stiffness.

2.5 Machine learning regression analyses

Machine learning methods are increasingly used in predicting the mechanical parameters of materials based on experimental data sets. A Gaussian process is a generalization of the Gaussian probability distribution and can be used as basis for sophisticated machine learning algorithms for classification and regression. In machine learning, Gaussian process regression (GPR) was developed out of neural networks research and is a Bayesian method for data regression or classification. Gaussian process models have become very popular for solving non-linear regression problems. They are known to be expressive, interpretable, avoid over-fitting, and to yield a high predictive performance in many thorough empirical comparisons [10], [11]. In this study, a GPR algorithm was used to perform a regression analysis on inputs and output results obtained from cyclic tests on hybrid connectors. Figure 7 features a schematic of the Gaussian process regression network. Squares represent observed variables and circles represent unknowns. x is a general input (predictor) variable, y is target output, and w are weights functions. Often a bias weight or offset is included to avoid over fitting. This noise assumption together with the model directly gives rise to the likelihood, the probability density of the observations given the parameters, which is factored over cases in the training set. Because of the marginalization property of GPR addition of further inputs, x, latent variables, f, and unobserved targets, $y*$, does not change the distribution of any other variables.

In the Bayesian formalism there is a need to specify a prior over the parameters, expressing the beliefs about the prior parameters before looking at the observations. In GPR, a zero mean Gaussian prior is used. Also, a shape of the function is set for the prior; in the case of this work, and exponential shape was used. Inference in the Bayesian linear model is based on the posterior distribution over the weights. The posterior combines the likelihood and the prior and captures everything known about the parameters. To make predictions for a test case, all possible parameter predictive distribution values are averaged and weighted by their posterior probability. Thus, the predictive distribution is given by averaging the output of all possible models regarding the Gaussian posterior. An inherent advantage of GPR processes is that the predicted output is a distribution, and not a number.

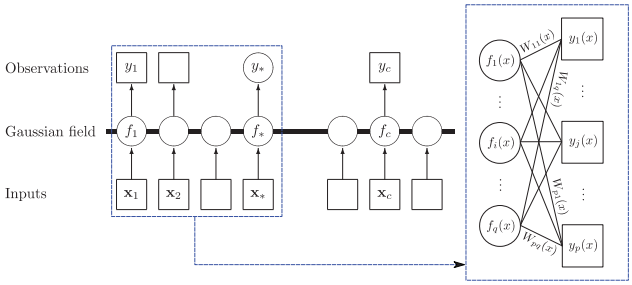

Figure 7: *The Gaussian process regression network. Adapted from [10], [12]*

In this work, the GPR was conducted under the software MATLAB, using the Regression Learner application. Two models were developed: one for the secant loading stiffness, and the other for the residual slip of the connector. The models were trained with normalized input parameters, as presented in Table 2.

Table 2*: Normalization of input parameters for the GPR learning algorithm*

	Actual values	**Normalized values**
variables		
CLT size (mm)	280, 340, 480	280, 340, 480
CLT grade	E, V	0, 1
Steel rod grade (strength class)	4.8, 8.8	0, 1
Rod diameter	20M, 24M, 30M	20, 24, 30
Grout-to-rod diameter ration	2x, 3x,4x	2, 3, 4
Covariates		
Horizontal eccentricity, d_1 (mm)	To be measured	Idem.
vertical eccentricity, d_2 (mm)		
Curing time for the grout (days)		

3 RESULTS

In this section, the mechanical characteristics evaluated based on the experiments are presented first; then, outputs from the Gaussian process regression ensue.

3.1 Cyclic performance of the connector

3.1.1 Secant loading stiffness and residual slip of the connectors

The box plots in Figure 8 provide a visualization of statistical information for two output data under consideration, namely the average secant loading stiffness at the last cycle of loading and the residual slip of the connector. The bottom and top of each box are the 25th and 75th percentiles of the data, respectively. Each box covers the interquartile interval, where 50% of the data is

found. The horizontal line in the middle of each box is the sample median. The thinner lines extending above and below each box represents whiskers, which go from the end of the interquartile range to the furthest observation within the whisker length [13]. This variation of the box and whisker plot restricts the length of the whiskers to a maximum of 1.5 times the interquartile range [14]. Data points that are outside this interval are represented as red points on the graph and considered potential outliers.

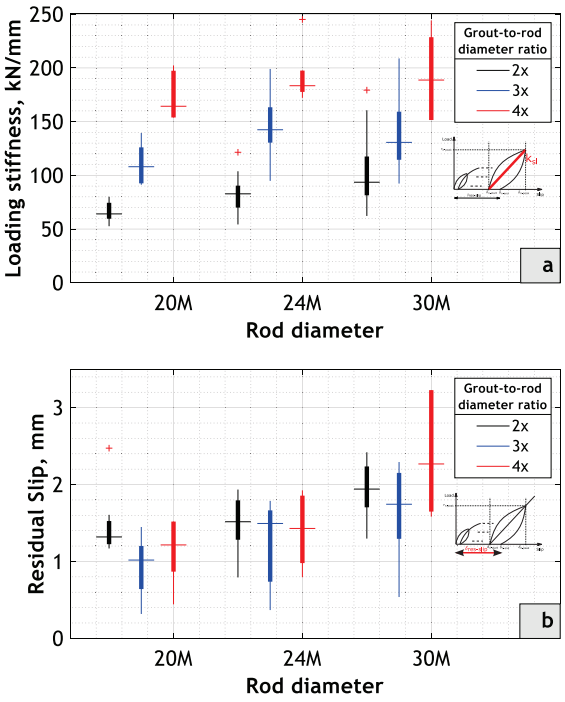

Figure 8: *Box plots of performance parameters. (a) loading stiffness, (b) residual slip. In black – grout to rod diameter ratio is 2; blue - grout to rod diameter ratio is 3; red - grout to rod diameter ratio is 4.*

A general trend is that the variability in loading stiffness increases with the grout diameter. The loading stiffness itself increases with both the rod diameter and grout diameter. As for the residual slip, once again, it is observed that the variability grows with the gout diameter. The effects of the rod and grout diameter on the residual slip are, however, less pronounced.

3.1.2 Hysteresis of connectors

The typical hysteresis of the connector is shown in Figure 9. This hysteresis corresponds to the connector tested with the loading diagram presented in Table 1 and Figure 3. In this plot, the load slip curves from monotonic tests are presented (Shulman and Loss [3], [4]). The hysteresis is represented by bold black, red, and blue lines. A switch in color in the hysteresis means a change of loading step. It was observed that the connector conserves it stiffness during cyclic loading (Figure 9). Additionally, the residual slip was observed to remain in moderate ranges. The premise that the hysteresis of the hybrid connector is contained within the monotonic load-slip curve is also validated. There appears to be a larger loop at the first cycle of the fourth load step: this was observed for all the connector variants tested. Lastly, a slight pinching is observed at the last load step. All tested connectors displayed a similar hysteresis pattern, with an observed residual slip between 40% and 60% of the maximum slip reached during the testing.

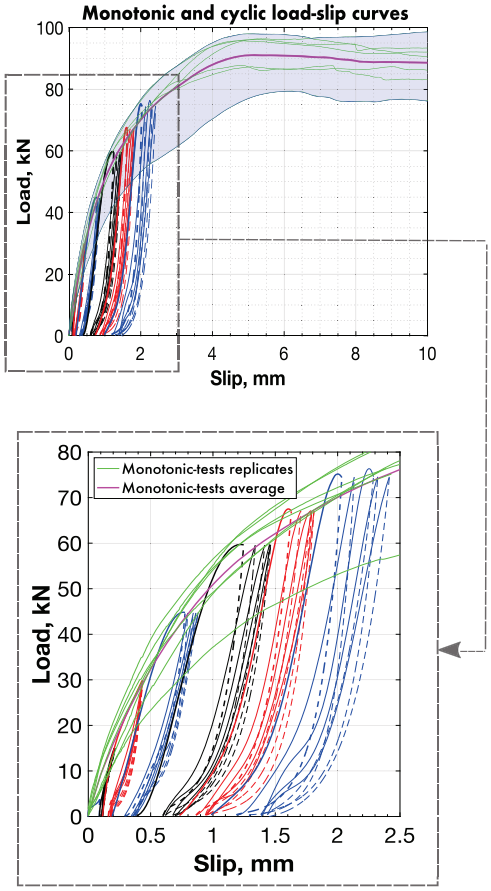

Figure 9: *Hysteresis of a specific tested connector arrangement (280–E–20M–4.8–2d)*

3.2 Gaussian process regression

Gaussian process regression (GPR) machine learning algorithm was used to develop predictive models for the secant loading stiffness and the residual slip of the connectors.

3.2.1 Variables importance scores

First, an F-test was used to determine the importance of each feature variable on the outputs. Figure 10 shows the feature importance scores.

https://doi.org/10.52202/069179-0174

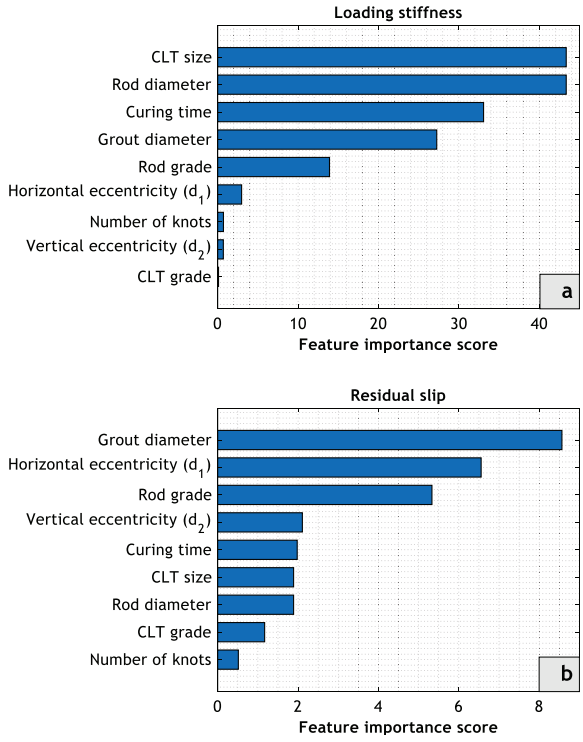

Figure 10: *Feature importance score obtained through the F-Test algorithm. (a) loading stiffness, (b) residual slip.*

It can be observed that the CLT size and the rod diameter have an equal importance score as far as the loading stiffness is concerned (Figure 10.a). This is because these two variables are perfectly correlated. 20M, 24M, and 30M rods were used on 280 mm, 340 mm, and 420 mm CLT blocks respectively. Because of this correlation, only the rod diameter was used for subsequent analyses. The curing time of the epoxy-based grout is third in the ranking of importance factors. Conversely, the CLT grade, the vertical eccentricity, and the number of knots in the face laminations of CLT were found to have very little effect on the secant loading stiffness of connectors.

As for the residual slip, it is observed that the grout diameter, the horizontal eccentricity, d_1, and the steel rod grade are the most significant parameters, with importance scores above 8, 6, and 5, respectively (Figure 10.b). The number of knots and CLT grade were found to have little effect on the residual slip of connectors

3.2.2 Training of GPR models

The GPR was executed twice: once for the secant loading stiffness, and the second time, the residual slip, leading to two trained models. In order to minimize the overfitting, 75% of the ninety data sets were randomly selected and used to train each model. Each model was then validated using the 25% remaining data. The root mean-square error as well as other parameters describing the performance of the algorithm are presented in Table 3. The scatter plots for predicted vs experimental data are presented in Figure 11.

Table 3: *Performance of the GPR learning algorithm*

	Secant Loading stiffness [kN/mm]	**Residual slip [mm]**
RMSE - *Validation*	26.007	0.5734
R-squared	0.70	0.57
Training time (obs/sec)	5700	6800
Prediction speed (sec)	3.353	2.2493

As can be seen from Table 3, the model for the secant loading stiffness presents a good validation root mean square error (RMSE), with a determination coefficient R-squared of 0.7 (this can be observed on Figure 11.a). The prediction speed for the 25% validation data was observed to be below the 3.50s.

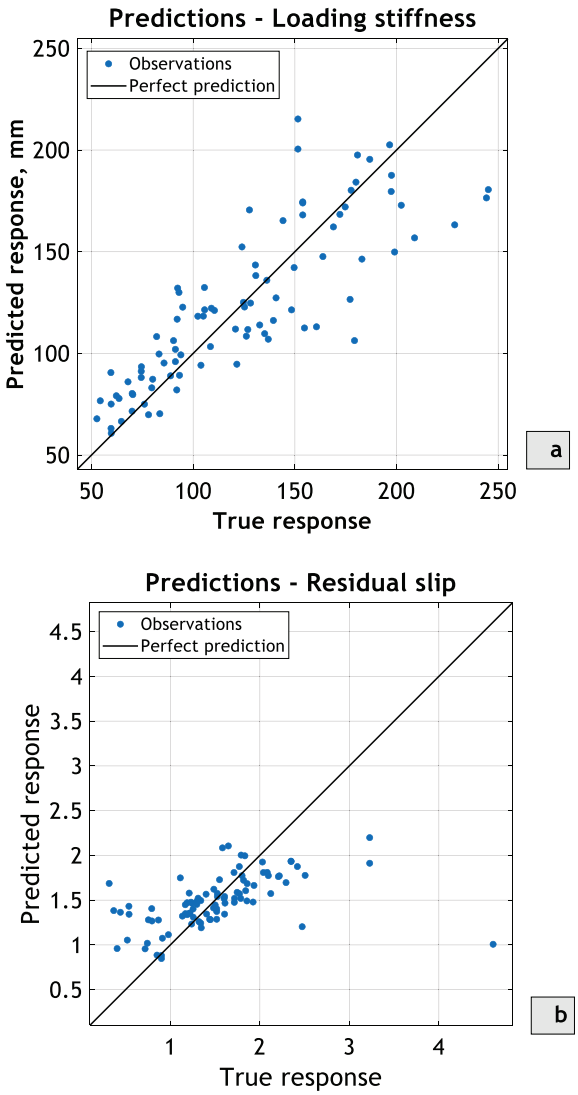

Figure 11: *Scatter plots of the predicted vs experimental data. (a) secant loading stiffness, (b) residual slip.*

The residual slip on the other hand was a little more complex to predict. The coefficient of determination for this model was obtained to be only 0.57 (this can be observed on Figure 11.b, with a few outliers on the lower

right corner of the plot). This can be due to the fact that other non-controlled variables may have a significant effect on the slip of connectors. For instance, the friction between the test apparatus and the specimens was not measured. In addition, the testing apparatus may have not stayed perfectly vertical all along the cycling process (Figure 4). In overall, the prediction speed was higher for the residual slip, with a prediction time of 2.25 s.

3.2.3 Response surface representations of trained GPR models

Using the developed models from the GPR learning algorithm, response surfaces were plotted in order to assess the overall effects of the most significant variables on the outputs.

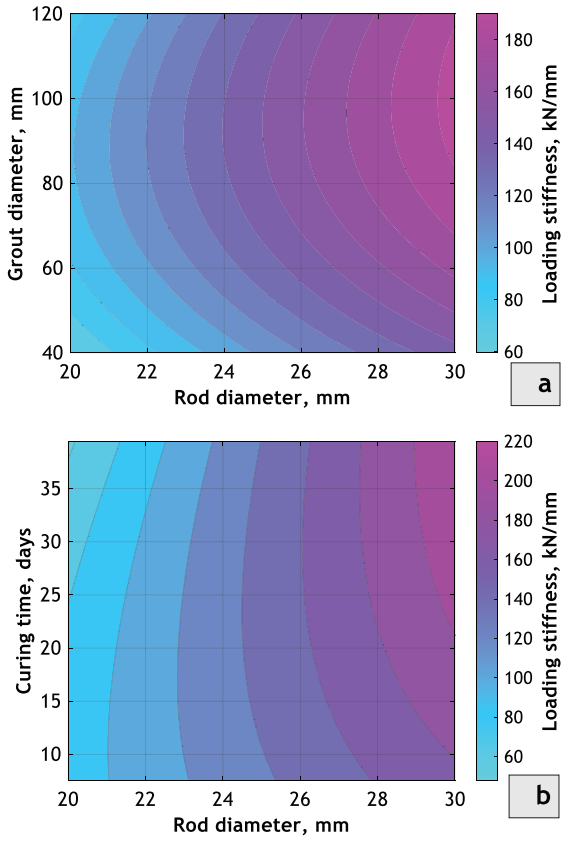

Figure 12: *Response surface of the predicted secant loading stiffness (units in kN/mm). (a) secant loading stiffness vs rod diameter & grout diameter, (b) secant loading stiffness vs rod diameter & curing time.*

First, the secant loading stiffness model was plotted, with variable parameters including diameters of rods and grout. With reference to Figure 12.a, it can be observed that the secant stiffness model captures the effects of the rod and grout diameters. Besides, it is shown that the grout diameter gradually has less impact on the secant loading stiffness as the rod diameter reaches larger values. In Figure 12.b, plots were drawn using the rod diameter and the curing time of the grout as variables. As a result, it can be seen that the curing time of the grout has larger effect on the secant loading stiffness as the rod diameter reaches extreme upper values.

Similarly, the residual slip was plotted, with variable parameters including the grout diameter and the horizontal eccentricity, d_1 (Figure 13.a). The residual slip appears to be lower with lower grout diameters. However, the value of horizontal eccentricity that minimizes the residual slip appears to be between 20 mm and 50 mm, and this value increases with the grout diameter. Results based on the grout diameter and the steel rod grade as variables are plotted in Figure 13.b. From these latter, it can be seen that there is a linear relation between inputs and outputs. The residual slip is minimized as the grout diameter decreases and the steel rod grade is kept at 1 (corresponding to 8.8 strength class).

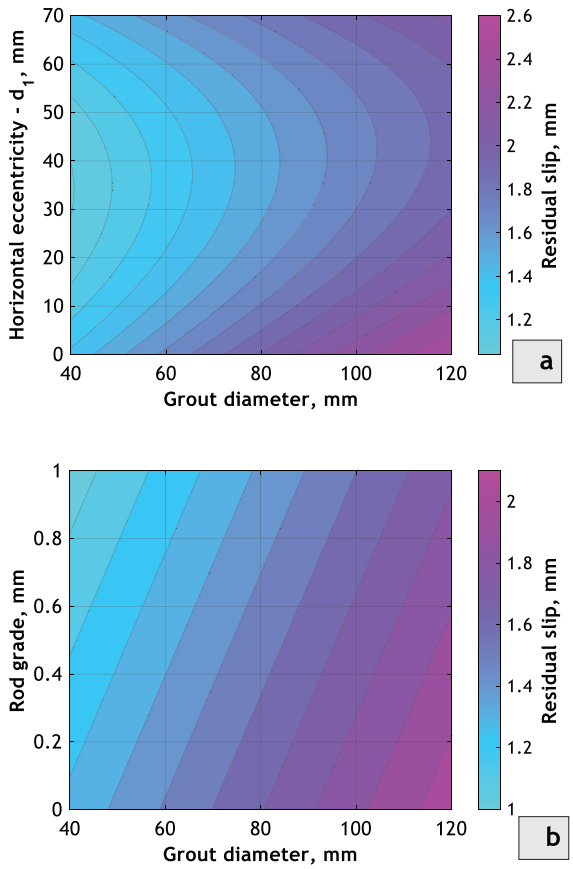

Figure 13: *Response surface of the predicted residual slip (units in mm). (a) residual slip vs & grout diameter & horizontal eccentricity, (b) residual slip vs grout diameter & steel rod grade.*

4 CONCLUSION

This work focused on the performance of a novel high-performance shear connector for mass-timber panels under quasi-static cyclic loading. In addition to assessing the experimental results, two models were developed using a Gaussian process regression machine learning

https://doi.org/10.52202/069179-0174

algorithm to determine the final secant loading stiffness and the residual slip of the connector. Based on the tests performed and analyses conducted, the following conclusions are at the forefront:

- The connector maintains its initial stiffness throughout the cyclic loading history
- The connector displays a relative residual deformation in the order of 50% at the end of the test.
- The most significant parameters influencing the secant loading stiffness are the rod diameter, curing time of the grout, and grout diameter. Whereas the most significant parameters for the residual slip are the grout diameter, the horizontal eccentricity and the steel rod grade.
- The Gaussian process regression algorithm yielded acceptable models for the prediction of the secant loading stiffness and the residual slip, with an r-squared value of 0.70 for the secant loading stiffness and 0.57 for the total residual slip.
- In overall, the results of this work contribute to an improved understanding of the connection under development and confirms the resilience of individual connectors under cyclic loads.

ACKNOWLEDGMENT

The research was funded by the Government of British Columbia through a FII Wood First grant and by the Natural Sciences and Engineering Research Council (NSERC) of Canada through the Discover Program grant number RGPIN-2019-04530, and Discovery Launch Supplement, grant number DGECR-2019-00265. Financial support from the Faculty of Forestry of the University of British Columbia through the Donald S. McPhee Fellowship and Dr. J. David Barrett Memorial Scholarship in Wood Science granted to Blériot Feujofack is gratefully acknowledged.

REFERENCES

[1] S. Breneman, T. Timmers, and D. Richardson, 'Tall wood buildings and the 2021 IBC: Up to 18 stories of mass timber', *American Wood Council*, no. 2019, p. 13, 2019.

[2] M. Geiser, M. Bergmann, and M. Follesa, 'Influence of steel properties on the ductility of doweled timber connections', *Construction and Building Materials*, p. 121152, Oct. 2020, doi: 10.1016/j.conbuildmat.2020.121152.

[3] Shulman, S., Loss, C., 2023, 'Performance of a Grout-Reinforced Hybrid Steel-Timber Shear Connection for Mass Timber Buildings', in: Walbridge, S., Nik-Bakht, M., Ng, K.T.W., Shome, M., Alam, M.S., El Damatty, A., Lovegrove, G. (Eds.), *Proceedings of the Canadian Society of Civil Engineering Annual Conference 2021*, Lecture Notes in Civil Engineering. Springer Nature Singapore, Singapore, pp. 341–352. https://doi.org/10.1007/978-981-19-0511-7_29.

[4] S. Shulman and C. Loss, 'High-performance grout-reinforced shear connectors for hybrid steel-cross-laminated timber building systems: Experimental study', *Journal of Building Engineering*, p. 106014, Feb. 2023, doi: 10.1016/j.jobe.2023.106014.

[5] S. Shulman, 'A deconstructable grout-reinforced hybrid shear connector for tall cross-laminated timber buildings', 2021.

[6] EN 12512, '12512: Timber structures-Test methods-Cyclic testing of joints made with mechanical fasteners', *English version of DIN EN*, no. 2001, p. A1, 2005.

[7] ASTM E2126, 'Standard test methods for cyclic (reversed) load test for shear resistance of vertical elements of the lateral force resisting systems for buildings', *ASTM E2126*, 2011.

[8] T. J. Sullivan, G. M. Calvi, and M. J. N. Priestley, 'Initial stiffness versus secant stiffness in displacement based design', in *13th World Conference of Earthquake Engineering (WCEE)*, 2004, no. 2888.

[9] R. Jockwer, D. Caprio, and A. Jorissen, 'Evaluation of parameters influencing the load-deformation behaviour of connections with laterally loaded dowel-type fasteners', *Wood Material Science & Engineering*, vol. 17, no. 1, pp. 6–19, 2022.

[10] C. E. Rasmussen and C. K. Williams, *Gaussian processes for machine learning*, vol. 1. Springer, 2006.

[11] M. Kuss, C. E. Rasmussen, and R. Herbrich, 'Assessing Approximate Inference for Binary Gaussian Process Classification.', *Journal of machine learning research*, vol. 6, no. 10, 2005.

[12] A. G. Wilson, D. A. Knowles, and Z. Ghahramani, 'Gaussian process regression networks', *arXiv preprint arXiv:1110.4411*, 2011.

[13] D. C. Montgomery and G. C. Runger, *Applied statistics and probability for engineers*. John wiley & sons, 2010.

[14] R. McGill, J. W. Tukey, and W. A. Larsen, 'Variations of box plots', *The american statistician*, vol. 32, no. 1, pp. 12–16, 1978.